Solvation Dynamics of the Hydrated Electron Depends on Its Initial Degree of Electron Delocalization†

Patanjali Kambhampati, Dong Hee Son, Tak W. Kee, and Paul F. Barbara*

Department of Chemistry and Biochemistry, The University of Texas at Austin, Austin, Texas 78712

Received: November 20, 2001

We investigate the time scale for hydrated electron solvation as a function of the initial configuration of the electron/water system. The experiments employ various 2-pulse and 3-pulse femtosecond pulse sequences that allow for controllable preparation of the various optically excited and precursor states of the equilibrated hydrated electron. We observe that the conduction band electron, which is produced by detrapping of the hydrated electron, has the slowest time scale for electron solvation with an average solvation time constant of 400 fs. In contrast, the solvation dynamics are significantly faster for electrons that are produced in "pre-solvated" environments. These latter examples include the excited p-state of the hydrated electron and the precursor states involved in UV femtosecond multiphoton ionization of water.

I. Introduction

The structure and dynamics of an excess electron in water, i.e., the hydrated electron,[1−9] is a unique prototype for a number of important dynamical processes including: (i) the relaxation of a nonequilibrium solvent configuration around a solute (solvation dynamics);[4,6−8,10−12] (ii) electron localization/delocalization in condensed systems;[13−15] (iii) autoionization in condensed phase;[16−19] and (iv) electronically nonadiabatic transitions.[20−23] Figure 1 summarizes the different experimental approaches[4,7,8,24,25] that have been used to prepare nonequilibrium electron/H_2O transient states. Ultrafast spectroscopy is used to monitor the nonequilibrium system as it relaxes to yield the final form, i.e., the equilibrated hydrated electron, e_{eq}. The electronic structure of e_{eq} is s-like in character. It is localized in a cavity ($r = 3$ Å) in the solvent, which is surrounded by ∼6 water molecules.[26]

The various nonequilibrium forms of the hydrated electron in Figure 1 involve an excitation of both electron and solvent degrees of freedom. One category includes the optically excited states of e_{eq}, namely e_p, e_{CB}', and e_{CB}''.[27] The optically excited states are produced by 1- or 2-photon excitation of e_{eq}, which itself is typically prepared by the multiphoton ionization of water with a prior UV laser in the experimental pulse sequence (not shown in Figure 1). A simple example is the optically prepared ($e_{eq} \rightarrow e_p$) e_p form, which consists of a set of three nondegenerate p-like states, that are trapped and localized in the same solvent cavity as their "parent" e_{eq}.[28]

An alternative category of nonequilibrium excess electrons in Figure 1 involve precursors to formation of e_{eq}, e.g., H_2O^*. H_2O^* signifies the water excited-state intermediate or intermediates in the near-threshold 2-photon (9.32 eV) ionization of water with 266 nm femtosecond excitation.[16−19,27,29,30] Another key precursor to the hydrated electron is the so-called conduction band, e_{CB}''', produced by exposing water to ionizing radiation.[31]

The different nonequilibrium forms are shown to scale in Figure 1, where the size of each state has been experimentally

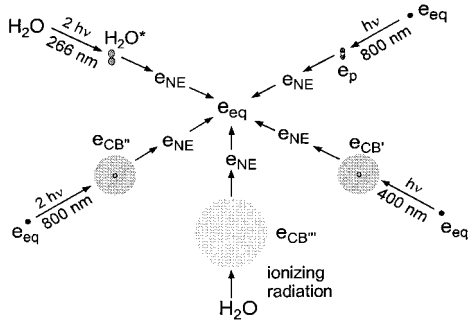

Figure 1. Outline of the various pathways for generating the precursors and other forms of the hydrated electron. See text for details. The different forms are shown to scale.

estimated from spatially sensitive measurements including e_{eq}/hole geminate recombination kinetics,[18] 3-pulse suppressed geminate recombination dynamics,[28] and chemical scavenging yield studies.[27] Of particular importance are the conduction band forms, which can either be precursor (e_{CB}''') or optically excited states of e_{eq} (e_{CB}', e_{CB}'').[8,22,28,32−35] The conduction band forms are delocalized over tens of angstroms. They lie above either the "vertical ionization threshold" (ca. 9−11 eV) for the photoionization of water, or, in the case of photodetrapping (e.g., $e_{eq} \rightarrow e_{CB}$), above the "vertical detrapping threshold".[18,29,32,36] It is important to emphasize that the conduction band electron is not significantly coupled to its original hole (ionization) or cavity (detrapping) site. During relaxation, it is trapped and solvated at a new solvent site.[8,28] Furthermore, the various conduction band forms are probably similar in structure and dynamics, but have distinct designations (e_{CB}', e_{CB}'', e_{CB}''') in this paper to emphasize that the experiments used to prepare them are very different and, as a result, may produce distinct electron and solvent configurations.

The electron migration length and electron/hole pair "escape yield" for H_2O^* is considerably smaller than that observed for conduction band electrons, consistent with the nonvertical nature of the ionization process. The 3-photon ionization of water at 400 nm (not shown in Figure 1) is similar to the 2-photon (9.32 eV) ionization of water and has been argued to have substantial p-state Rydberg character.[27] We designate the precursor in the

† Part of the special issue "Noboru Mataga Festschrift".

* To whom correspondence should be addressed. E-mail: p.barbara@mail.utexas.edu.

10.1021/jp014291p CCC: $22.00
Published on Web 01/23/2002

400 nm multiphoton ionization as H_2O^{**}, although this channel has mixed contribution from 3 and 3+1 photon ionization that complicated discussions on this electron precursor.[18,19,29] It has also been argued that H_2O^* and H_2O^{**} are ionized by charge transfer to rare existing solvent cavities in water that are thermally "presolvated," allowing for sub-threshold ionization.[16−18]

In this paper, we use femtosecond pump−probe spectroscopy to determine to what extent the time scale for equilibration of the hydrated electron is a function of how it is prepared. The experiments employ different types of femtosecond 2- and 3-pulse sequences with time resolution in the range of 50−120 fs and probe wavelength in the visible and near-infrared region. Due to the short lifetime of most of the initially formed states (H_2O^*, H_2O^{**}, e_{CB}', e_{CB}'') and the expectation that most of the states absorb at wavelength >2 μm,[22,33−35] our "observation window" essentially begins with e_p and $e_{s,NE}$ (s-state form with a nonequilibrium solvent configuration).

The main result of this paper is that the time scale for initial stages of hydrated electron relaxation (e_p, $e_{s,NE} \rightarrow e_{eq}$) is correlated to the extent of delocalization of the initially prepared species. The observed relaxation reported herein is slowest for the conduction band (e_{CB}', e_{CB}'') electrons and fastest for the "pre-solvated" H_2O^*, H_2O^{**}, and e_p. These results lead to a new level of understanding of relationship of the different types of experiments on the hydrated electron. In addition, the new results have important implications on understanding the relationship between photoionization of water with femtosecond UV pulse[4,6] and radiolysis of water with ionizing radiation.[37,38]

II. Experimental Section

The laser system used in these experiments is composed of a home-built Kerr lens mode locked Ti:sapphire oscillator pumped by a Nd:YVO_4 laser and a Ti:sapphire multipass amplifier pumped by a Nd:YLF laser. A detailed description of the laser system can be found elsewhere.[8] Briefly, <20 fs pulses, centered at 800 nm and generated from the oscillator, were subsequently stretched and amplified to give 35 fs, 0.4 mJ pulses at 1 kHz after compression.

The amplified femtosecond laser beam was divided into four beams. The first and second beams were used to generate the 266 nm photoionization pulses. The first beam was used to produce the second harmonic at 400 nm in a BBO crystal which was then mixed with the second 800 nm beam in another BBO crystal to produce the 266 nm beam. The third beam of fundamental 800 nm light was used for the pump pulse. For the 400 nm pump experiments, the 800 nm light was doubled in a BBO crystal. The fourth beam of fundamental 800 nm light was used to produce white light continuum in a sapphire crystal. The continuum was used to probe the transient optical density of the hydrated electron after filtering and compensation for optical dispersion in a fused silica prism pair.

The pulse widths for the 800, 400, and 266 nm pulses were respectively, 35, 60, and 110 fs. The instrument response function for photoionization/probe experiment was 120 fs fwhm. For the photoionization/pump/probe configuration, the cross-correlation time between the probe and the pump pulse was 50 and 70 fs for 800 and 400 nm pump pulses, respectively. The sample solutions were continuously flowed through a 300 μm jet nozzle to avoid repeated exposure of the same region of the sample to the laser pulses.

III. Results and Discussion

The well-known absorption spectrum of the fully equilibrated hydrated electron e_{eq} is reproduced in Figure 2a.[39] The main

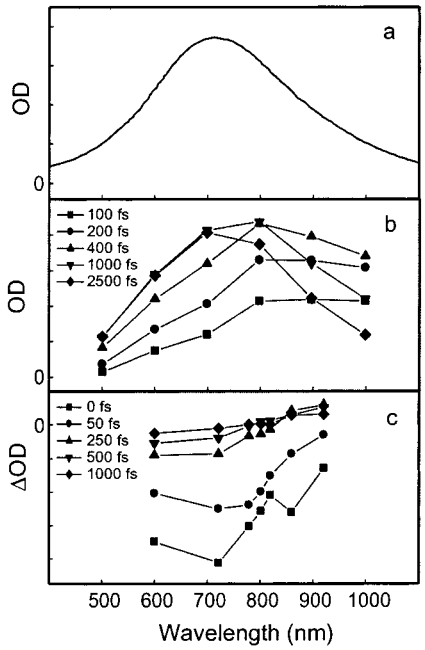

Figure 2. Static and transient spectra of the hydrated electron. (a) Absorption spectrum of the solvated electron adapted from Jou et al.[39] (b) Transient spectrum of the photoinjected electron adapted from Bradforth et al.[2] (c) Transient spectrum of the preequilibrated hydrated electron adapted from Yokoyama et al.[8]

portion of the spectrum and most of the oscillator strength has been assigned to the s → p transition.[20,34] Recent results show, however, that at short wavelengths (e.g., 400 nm) a transition ($e_{eq} \rightarrow e_{CB}'$) occurs between e_{eq} and the conduction band with unity quantum yield of the conduction band electrons.[40]

Typical spectra reflecting the formation and relaxation of $e_{s,NE}$ are shown in Figure 2. Figure 2b displays data reproduced from the work of Bradforth et al.[2] on the 2-photon ionization of water at 266 nm, via a H_2O^* precursor. The hydrated electron absorption of the nonequilibrium forms blue-shifts toward the visible as trapping and relaxation occurs on the 100−1000 fs time scale.[4] The $e_{s,NE}$ spectrum is due primarily to the s → p transition and further evolves within 1−2 ps into the fully relaxed e_{eq} spectrum. Finally, the early absorption data may be partly due to trapping a portion of the electrons in the p-state, $H_2O^* \rightarrow e_p$, as discussed in a later section of this paper and elsewhere.[2]

The complex multi-time-scale relaxation dynamics of $e_{s,NE}$ can be quantified by recording the transient parameters at an individual probe wavelength or by globally fitting the entire spectrum in the visible and near-infrared region to obtain a time dependent width, peak frequency, or other characteristic parameters. In this paper we use the single wavelength approach because it is less time-consuming and less susceptible to experimental uncertainties due to temporal dispersion of the probe pulse. Figure 3a and 3e display 2-pulse photoionization/probe transients probed at 720 and 1000 nm for $e_{s,NE}$ produced from 2-photon ionization of water with 266 nm, 110 fs pulses (H_2O^*). Figure 3b and 3f shows transients due to a mixture of 3-photon and 3+1 photon ionization with 400 nm, 60 fs pulses (H_2O^{**}). A very weak pulse-limited rise and decaying absorption in the visible is also observed and may be associated with absorption of a very short-lived H_2O^+.[41−43] Probing at 1000 nm in the near-infrared region monitors a higher-energy nonequilibrium form of the hydrated electron than that monitored at shorter wavelengths, e.g., 720 nm. The data at 1000 nm is more sensitive to earlier processes, but probably is not at

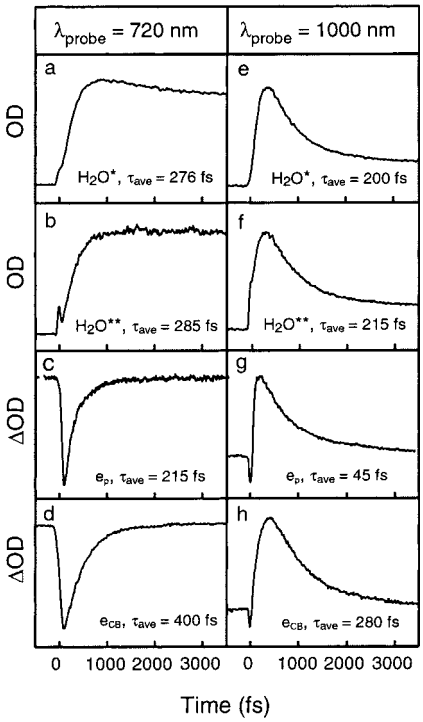

Figure 3. Femtosecond transient absorption data of the various precursors and forms of the hydrated electron at 720 (a−d) and 1000 nm (e−h) probe.

TABLE 1: Migration lengths (l_m)[a] and Average Solvation Times (τ_{avg})[b] for Different Forms and Precursors to the Hydrated Electron Measured at 720 and 1000 nm Probe Wavelengths

		τ_{avg} (fs)	
state	l_m (Å)	720 nm	1000 nm
e_p	<3	215	45[c]
H_2O^*	8.5	276	200
H_2O^{**}	14	285	215
e_{CB}	>35	400	280[c]

[a] Migration lengths were reported in Reference 40. [b] Solvation times reported from single wavelength data. The data are fit to a multiexponential function and the average solvation time is calculated by $\tau_{ave} = i\ A_i\tau_i / i\ A_i$ where A_i is the amplitude for τ_i. [c] Solvation time reported for only appearance portion of the kinetics, i.e., kinetic components with positive A_i values. The amplitudes for these cases have been normalized to reflect only the positive amplitude contributions to the kinetics.

sufficiently long wavelength to cleanly monitor the electron trapping dynamics. For the 1000 nm data, we focus exclusively on the appearance kinetics of the signal, which reflects the formation kinetics of the $e_{s,NE}$.[2,8] For the 720 nm transient, which only involves appearance kinetics and no decay, the average time scale for appearance reflects the time scale for the electron solvation to form the fully relaxed species. The different relaxation times are summarized in Table 1.

The spectral dynamics due to hydrated electron relaxation for the optically excited states, e_p, e_{CB}', and e_{CB}'', are recorded by a 3-pulse experiment incorporating photoionization, photoexcitation, and variably delayed probe pulses. Typically, the excitation pulse is delayed a sufficiently long time (e.g., 20 ps) after the photoionization pulse such that the excitation pulse excites a fully equilibrated electron, e_{eq}. The transient absorption data (Figure 2c and Figure 3c,3d,3g,3h) recorded by this technique essentially correspond to a ground-state-depletion/recovery experiment. The optical density is therefore in the form of a "bleach" due to ground-state depletion followed by recovery

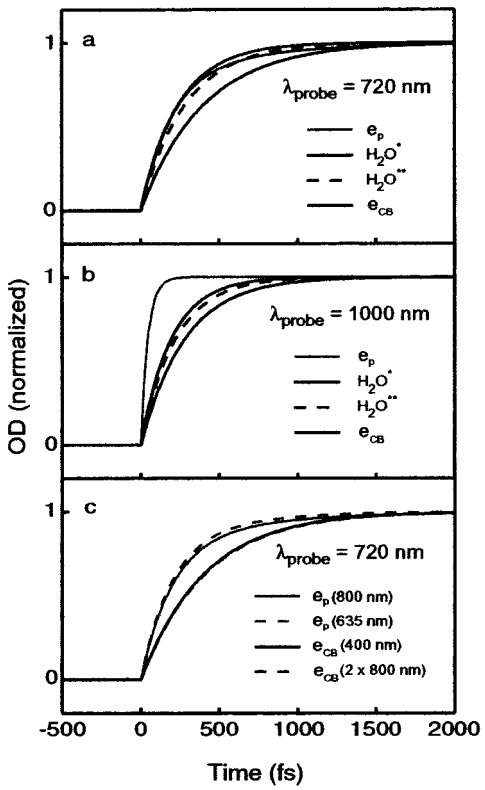

Figure 4. Fits of the hydrated electron transient absorption data. Panel (a) and (b) show that the solvation dynamics are dependent on the initial degree of delocalization. Panel (c) shows that excess nuclear energy does not alter the solvation dynamics, whereas it is the electronic state that does. The traces are reconstructed from the fit parameters of the experimental data. The fits were used due to different time resolution in each of these experiments and the need to correct for geminate recombination. The contribution from geminate recombination is corrected for by dividing the experimental kinetic trace with calculated geminate recombination kinetic trace. Corrected kinetic trace shows about 10% slower dynamics than uncorrected one.

of the bleach and spectral shifting due to electronic relaxation (e.g., p → s) and solvation in the p- and s-states.[5,7,8] By varying the wavelength[40] and pulse energy[28] of the excitation pulse, it is possible to selectively excite the equilibrated hydrated electron to the p-state or the conduction band.

Figure 3c−3d and 3g−3h shows examples of 720 and 1000 nm transients from the 3-pulse experiments with excitation to e_p and e_{CB} respectively. Data of this type can be analyzed to extract analogous time constants to those discussed above for the 2-pulse experiments on the precursor states. The time scale for hydrated electron relaxation for the different precursor states and excited states are compared in Table 1 and Figure 4. To analyze and fit the H_2O^* and H_2O^{**} precursor data to extract the relaxation time-scales, it was necessary to correct the transients for the small amount of e_{eq}/hole geminate recombination that occurs during the relaxation process.

The clear trend in these data is that the time scale for relaxation of a conduction band electron is considerably slower than the electrons produced via H_2O^*, H_2O^{**} or e_p. One possible explanation for this result is that the more quickly relaxing cases involve electron species that are already partially solvated. For excitation to e_p, the cavity surrounding the electron is already fully equilibrated in the s-state before excitation. Thus, during the excitation pulse (~40 fs) and during the p-state decay (50 or 300 fs depending on assignment), the slow solvent modes are essentially frozen. Likely candidates for the slow motion include diffusive rotational and translational modes of water.[11,44]

A particularly fast rise of the signal for e_p at 1000 nm (Figure 3g) may be partially due to immediate population of the p-state by photoexcitation, or alternatively to a very short e_p lifetime. (The 3-pulse experiments with excitation to e_{CB} is related to an earlier report of conduction band 1-photon detrapping with 300 nm excitation.[45] These latter measurements had insufficient time resolution to distinguish among the different types of electron relaxation reported herein).

For the excited states of water, H_2O^*, H_2O^{**}, the existence of a pre-solvated structure is consistent with the proposed near-threshold photoionization process, i.e., $H_2O^* \rightarrow e_{eq}$.[16,18,29,46] The electron ejection process has been assigned to charge transfer from H_2O^* to preexisting deep trap sites or solvent cavities. The thermally prepared sites already have a structure that is favorable for electron solvation. In other words, the preexisting hydrated electron sites are "pre-solvated."

The proposed dependence of electron solvation time scales on the degree of pre-solvation is also reflected in the observed correlation of solvation times with electron migration length (l_m), as shown in Table 1. The electron migration length of the hydrated electron species that precedes the formation of $e_{s,NE}$ is closely related to local solvent configuration. For e_p, the small migration length is a consequence of the localization of the electron in a pre-solvated cavity that was formed around the initial e_{eq} from which e_p was prepared by optical excitation.[28] For H_2O^* and H_2O^{**} the small migration length (as compared to l_m for the conduction band) is consistent with the interpretation of H_2O^* and H_2O^{**} as diffuse, locally excited states of water.[27] As mentioned above, H_2O^* and the 3-photon-400 nm component of H_2O^{**} are below the conduction band of water and require preexisting, pre-solvated cavities in water.

The slow time scales for relaxation of the conduction band electrons, e_{CB}'(1-photon-400 nm) and e_{CB}''(2-photon-800 nm), are presumably due to electron localization, trapping, and solvation in water sites that have a relatively small amount of pre-solvation. Simulations show that the equilibrium concentration (or density) of sites with a small degree of pre-solvation is much higher than that for more localized, "deep" pre-solvated sites.[47] The conduction band electron has a sufficiently large migration length and total energy to sample the plentiful "shallow" preexisting electron trap sites in water.

The difference between the solvation time scales for a pre-solvated electron (e.g., e_p) versus a conduction band electron is especially relevant to the optically prepared electron species in the 3-pulse experiments[5,7,8,12,45]. The single photon excitation ($e_{eq} \rightarrow e_p$) experiments with excitation at 800 nm (1.55 eV), 635 nm (1.95 eV), and 720 nm (1.72 eV, not shown here) have identical time scales for electron solvation within experimental error. Thus, significant changes in the excitation energy have little dynamic consequences as long as the same localized state (e_p) is produced. In contrast, with 400 nm (3.10 eV) excitation a highly delocalized conduction band state is produced with a large migration length[40] and a relatively slow solvation time scale. Furthermore, the two methods for producing the conduction band (400 nm 1-photon[40] or 800 nm 2-photon[8,28]) have identical solvation time scales.

An additional complex issue involving the relaxation mechanism of the hydrated electron is the potential role of the p-state electron. Molecular dynamics simulations[35] suggest that about 50% of conduction band electrons should proceed through the p-state

$$e_{CB} \rightarrow e_p \rightarrow e_{s,NE} \rightarrow e_{eq} \quad (1)$$

where $e_{s,NE}$ in this case is nonequilibrium form of the ground state, e_{eq}. The other 50% of the conduction band population is predicted to proceed directly to s-state, as follows

$$e_{CB} \rightarrow e_{s,NE} \rightarrow e_{eq} \quad (2)$$

It would be an important breakthrough in hydrated electron research to definitively determine whether the p-state is indeed populated in conduction band relaxation.

To address this issue, it is useful to consider how p-states are involved in the relaxation of the other nonconduction band electrons and electron precursors. Of course, the 3-pulse experiments that exclusively produce the p-state (e.g., 800 nm 1-photon excitation) should be particularly revealing. For these experiments, the time-dependent evolution of the spectrum has been assigned to a complex combination of p-state to s-state nonadiabatic relaxation with adiabatic relaxation in both the s-state and p-state.[7,8] The different contributions to the dynamics have similar spectral manifestation (time-dependent blue shift in the spectrum) and are difficult to unravel. The three major time scales for spectral dynamics of e_p (79 fs, 263 fs, 630 fs) have been assigned respectively to excited-state relaxation, p $\rightarrow$ s internal conversion, and ground-state solvation.[8] Furthermore, this interpretation is based on the assumption that the excited p-state absorbs in the 800 nm region. This latter assignment is consistent with observation that 2-photon 800 nm absorption effectively produces e_{CB}''.[8,28]

It is tempting to use the spectroscopy of e_p from the $e_{eq} \rightarrow e_p$ 3-pulse experiments to evaluate whether p-state electrons are indeed formed in the 3-pulse conduction band experiment. The data in Figure 4 reveal that the conduction band data are missing the short time-scale dynamics in the 720 nm region that has been assigned to p-state absorption and relaxation. Does this indicate that few p-state electrons are formed during relaxation of conduction band electrons? Unfortunately, the answer is not completely clear, because the p-state in the two experiments may absorb in different wavelength regions due to the different nonequilibrium solvent configurations.

It is unclear whether the p-state is an intermediate in UV photoionization experiments. For this type of experiment the p-state may be formed from the photoejection process, as follows

$$H_2O^* \rightarrow e_p \rightarrow e_{s,NE} \rightarrow e_{eq} \quad (3)$$

This is in parallel with the direct formation of $e_{s,NE}$

$$H_2O^* \rightarrow e_{s,NE} \rightarrow e_{eq} \quad (4)$$

Previous results[4,48] suggesting that both processes (eqs 3 and 4) occur in parallel are consistent with the similar dynamics reported herein for the genuine p-state experiment (3-pulse 800 nm excitation) and the 2-pulse 266 nm experiments (see Figure 2 for example). Although this seems to argue that e_p is formed from H_2O^*, others argue that the H_2O^* ionization route (7$-$9.32 eV) is significantly below the vertical conduction band threshold (9$-$11 eV),[18,19,29,32,36,49] which seems to suggest that the lower energy channel, eq 4, should be more favorable. The escape yield is constant from 7 to 9.32 eV, which indicates that this energy range produces the same species.[18] An energy of 7 eV is clearly below the conduction band edge suggesting $e_{s,NE}$ formation. The state produced by MPI cannot be clearly resolved with this experiment, however, as we cannot distinguish e_p and $e_{s,NE}$ by dynamics alone.

It is interesting to contrast the various experiments describe herein with the analogous time-resolved experiment with ionizing radiation, i.e., pulse radiolysis.[24,25,37] Unfortunately, pulse radiolysis does not have sufficient time resolution to

directly examine the time scale for electron solvation. On the basis of indirect measurements including slower track kinetics, yield studies with electron scavengers, theoretical modeling, etc, it is generally assumed that ionization proceeds through a conduction band electron, e_{CB}''', shown in Figure 1. The conduction band in radiation chemistry, e_{CB}''', is known to have a migration length of 52 Å.[50,51] It is interesting to compare e_{CB}''' to the two forms of the conduction band produced by the 3-pulse sequence. The latter species have an observed lower limit to the migration length of 35 Å and as such may be electronically indistinguishable from the species produced in radiolysis. The radiolysis and 3-pulse sequence species differ however with regard to the partner for electron. In radiolysis, a H_2O^+ hole which fragments rapidly, is located at the center of the conduction band. In the 3-pulse experiment with 400 nm excitation, an empty cavity is located at the center of conduction band due to the detrapping process. The cavity itself would be expected to disappear on the ~1 ps due to solvent motion. Also, because the 3-pulse experiment involves an initial ionization step that produces a hole, the conduction band produced in the 3-pulse experiments actually has both a hole and a solvent cavity at early times but only a hole at times much greater than 1 ps.

It is important to note, however, that the near-threshold 2-pulse photoionization/probe experiment does not produce a conduction band electron (as mentioned above) and as such is not analogous to the major mechanism of ionization in radiolysis, although some of the electrons in radiolysis may be produced by H_2O^* like species. It would be useful to develop a 2-pulse technique that will directly produce conduction band electrons, but this might require shorter wavelength femtosecond sources and more complex multicolor multiphoton ionization schemes to strongly favor an above threshold ionization.

IV. Conclusions and Summary

The hydrated electron solvation dynamics were measured for the different precursor states and optically excited e_{eq}. The observed relaxation corresponds to the latter states (>100 fs) of the relaxation as the hydrated electron becomes fully equilibrated. Many of the experiments described in this paper employ a femtosecond 3-pulse sequence allowing for controllable preparation and monitoring of different nonequilibrium forms of the hydrated electron including the highly delocalized conduction band forms, e_{CB}' and e_{CB}''. It is observed that the conduction band electron forms exhibit significantly slower relaxation dynamics than the p-state electron and precursor states (e_p, H_2O^*, H_2O^{**}) that have an initially localized configuration in a pre-solvated solvent environment. The results offer new insight into the differences in structure and dynamics among the various nonequilibrium forms of the hydrated electron. The results also offer new insight into the fundamental difference between the UV photoionization of water and radiolysis.

Acknowledgment. We gratefully acknowledge support of this research by the Basic Energy Sciences Program of the Department of Energy and the Robert A. Welch Foundation.

References and Notes

(1) Kloepfer, J. A.; Vilchiz, V. H.; Lenchenkov, V. A.; Germaine, A. C.; Bradforth, S. E. *J. Chem. Phys.* **2000**, *113*, 6288.

(2) Vilchiz, V. H.; Kloepfer, J. A.; Germaine, A. C.; Lenchenkov, V. A.; Bradforth, S. E. *J. Phys. Chem. A* **2001**, *105*, 1711.

(3) Anderson, N. A.; Hang, K.; Asbury, J. B.; Lian, T. *Chem. Phys. Lett.* **2000**, *329*, 386.

(4) Shi, X.; Long, F. H.; Lu, H.; Eisenthal, K. B. *J. Phys. Chem.* **1996**, *100*, 11 903.

(5) Assel, M.; Laenen, R.; Laubereau, A. *J. Phys. Chem. A* **1998**, *102*, 2256.

(6) Assel, M.; Laenen, R.; Laubereau, A. *Chem. Phys. Lett.* **2000**, *317*, 13.

(7) Silva, C.; Walhout, P. K.; Yokoyama, K.; Barbara, P. F. *Phys. Rev. Lett.* **1998**, *80*, 1086.

(8) Yokoyama, K.; Silva, C.; Son, D. H.; Walhout, P. K.; Barbara, P. F. *J. Phys. Chem. A* **1998**, *102*, 6957.

(9) Baltu?ka, A.; Emde, M. F.; Pshenichnikov, M. S.; Wiersma, D. A. *J. Phys. Chem. A* **1999**, *103*, 10 065.

(10) Rossky, P. J.; Simon, J. D. *Nature* **1994**, *370*, 263.

(11) Horng, M. L.; Gardecki, J. A.; Papazyan, A.; Maroncelli, M. *J. Phys. Chem.* **1995**, *99*, 17 311.

(12) Emde, M. F.; Baltuska, A.; Kummrow, A.; Pshenichnikov, M. S.; Wiersma, D. A. *Phys. Rev. Lett.* **1998**, *80*, 4645.

(13) Ge, N.-H.; Wong, C. M.; Lingle, R. L., Jr.; McNeill, J. D.; Gaffney, K. J.; Harris, C. B. *Science* **1998**, *279*, 202.

(14) Lehr, L.; Zanni, M. T.; Frischkorn, C.; Weinkauf, R.; Neumark, D. M. *Science* **1999**, *284*, 635.

(15) Rosenblit, M.; Jortner, J. *Phys. Rev. Lett.* **1995**, *75*, 4079.

(16) Rottke, H.; Trump, C.; Sandner, W. *J. Phys. B* **1998**, *31*, 1083.

(17) Lee, M. T.; Wang, K.; McKoy, V.; Machado, L. E. *J. Chem. Phys.* **1992**, *97*, 3905.

(18) Crowell, R. A.; Bartels, D. M. *J. Phys. Chem.* **1996**, *100*, 17 940.

(19) Bartels, D. M.; Crowell, R. A. *J. Phys. Chem.* **2000**, *104*, 3349.

(20) Schwartz, B. J.; Rossky, P. J. *J. Chem. Phys.* **1994**, *101*, 6917.

(21) Prezhdo, O. V.; Rossky, P. J. *J. Chem. Phys.* **1997**, *107*, 5863.

(22) Staib, A.; Borgis, D. *J. Chem. Phys.* **1995**, *103*, 2642.

(23) Neria, E.; Nitzan, A.; Barnett, R. N.; Landman, U. *Phys. Rev. Lett.* **1991**, *67*, 1011.

(24) Bartels, D. M.; Cook, A. R.; Mudaliar, M.; Jonah, C. D. *J. Phys. Chem. A* **2000**, *104*, 1686.

(25) Kenney-Wallace, G. A.; Jonah, C. D. *J. Phys. Chem.* **1982**, *86*, 2572.

(26) Prezhdo, O. V.; Rossky, P. J. *J. Phys. Chem.* **1996**, *100*, 17 094.

(27) Kee, T. W.; Son, D. H.; Kambhampati, P.; Barbara, P. F. *J. Phys. Chem. A* **2001**, *105*, 8434.

(28) Son, D. H.; Kambhampati, P.; Kee, T. W.; Barbara, P. F. *J. Phys. Chem. A* **2001**, *105*, 8269.

(29) Sander, M. U.; Gudiksen, M. S.; Luther, K.; Troe, J. *Chem. Phys.* **2000**, *258*, 257.

(30) Sander, M. U.; Luther, K.; Troe, J. *J. Phys. Chem.* **1993**, *97*, 11 489.

(31) Jonah, C. D. M., M. S.; Miller, J. R.; Hart, E. J. *J. Phys. Chem.* **1976**, *80*, 1267.

(32) Coe, J. V.; Earhart, A. D.; Cohen, M. H.; Hoffman, G. J.; Sarkas, H. W.; Bowen, K. H. *J. Chem. Phys.* **1997**, *107*, 6023.

(33) Barnett, R. B.; Landman, U.; Nitzan, A. *J. Chem. Phys.* **1989**, *90*, 4413.

(34) Schnitker, J.; Motakabbir, K.; Rossky, P. J.; Friesner, R. *Phys. Rev. Lett.* **1988**, *90*, 456.

(35) Murphrey, T. H.; Rossky, P. J. *J. Chem. Phys.* **1993**, *99*, 515.

(36) Goulet, T.; Bernas, A.; Ferradini, C.; Jay-Gerin, J. P. *Chem. Phys. Lett.* **1990**, *170*, 492.

(37) Saleh, N.; Flippo, K.; Nemoto, K.; Umstadter, D.; Crowell, R.; Jonah, C. D.; Trifunac, A. D. *Rev. Sci. Instrum.* **2000**, *71*, 2305.

(38) Kenney-Wallace, G. A.; Jonah, C. D. *J. Phys. Chem.* **1982**, *86*, 2572.

(39) Jou, F.-Y.; Freeman, G. R. *J. Phys. Chem.* **1979**, *83*, 2385.

(40) Son, D. H.; Kambhampati, P.; Kee, T. W.; Barbara, P. F. *Chem. Phys. Lett.* **2000**, *342*, 571.

(41) Long, F. H.; Lu, H.; Eisenthal, K. B. *Phys. Rev. Lett.* **1990**, *64*, 1469.

(42) Das, B.; Farley, J. W. *J. Chem. Phys.* **1991**, *95*, 8809.

(43) Gauduel, Y. P., S.; Migus, A.; Antonetti, A. *Chem. Phys.* **1990**, *149*, 1.

(44) Jimenez, R.; Fleming, G. R.; Kumar, P. V.; Maroncelli, M. *Nature* **1994**, *369*, 471.

(45) Assel, M.; Laenen, R.; Laubereau, A. *J. Chem. Phys.* **1999**, *111*, 6869.

(46) Sander, M. U.; Luther, K.; Troe, J. *J. Phys. Chem.* **1992**, *97*, 11 489.

(47) Schnitker, J.; Rossky, P. J.; Kenney-Wallace, G. A. *J. Chem. Phys.* **1986**, *85*, 2986.

(48) Webster, F. J.; Schnitker, J.; Friedrichs, M. S.; Friesner, R. A.; Rossky, P. J. *Phys. Rev. Lett.* **1991**, *66*, 3172.

(49) Thomsen, C. L.; Madsen, D.; Keiding, S. R.; Thogersen, J.; Christiansen, O. *J. Chem. Phys.* **1999**, *110*, 3453.

(50) Pimblott, S. M. **2000**, private communication.

(51) Pimblott, S. M.; Laverne, J. A. *J. Phys. Chem. A* **1997**, *101*, 5828.